Trafficking SNARE SYP132 Partakes in Auxin-Associated Root Growth[1][OPEN]

Dear Editor,

In plants, cellular membrane traffic coordinates osmotic cell expansion and ion transport for cellular homeostasis and growth (Karnik et al., 2017). The plant hormone auxin regulates growth responses in roots (Haswell, 2003; Enami et al., 2009; Monshausen et al., 2011; Ichikawa et al., 2014); even so, little is understood about auxin-mediated control of membrane traffic in this tissue. Recently we identified as a target for hormone regulation a soluble *N*-ethylmaleimide-sensitive factor-attachment protein receptor (SNARE) protein, the Syntaxin of Plants 132 (SYP132). SYP132 is a member of the superfamily of proteins mediating vesicle fusion. Auxin modulates *SYP132* transcript levels and SYP132 protein expression to influence membrane traffic associated with this SNARE (Xia et al., 2019). Unusual for a secretory SNARE, SYP132 is involved in the endocytosis of plasma membrane H^+-ATPase proteins and reduces their density and activity at the plasma membrane, thereby suppressing H^+ transport in the shoots (Xia et al., 2019). In roots, the SNAREs SYP132 and SYP123 are both essential to the plant. SYP123 accumulates at the growing root hair tip. By contrast, SYP132 distributes evenly throughout the root as well as the shoot, suggesting that this SNARE has a constitutive role in growth (Enami et al., 2009; Ichikawa et al., 2014).

We explored SYP132 in root elongation and auxin-dependent growth responses in Arabidopsis (*Arabidopsis thaliana*) taking advantage of tools developed previously (Xia et al., 2019). We conclude that, in roots, auxin leads to an initial decrease, followed by an increase in SYP132 protein expression. Under gravitropic stimulation, this temporal behavior closely matches the second phase of differential auxin-induced cell expansion, which drives root bending (Guilfoyle et al., 1992; Band et al., 2012). We also observed that SYP132 over-expression masked the dose-dependent response in root growth to auxin and as in shoots (Xia et al., 2019), it also reduced root growth. In gravistimulated roots, SYP132 expression was differentially regulated at the top and bottom flanks of the organ. As such, SYP132 protein expression has an inverse correlation with cell growth. Thus, we identified that the SNARE SYP132 and its regulation by the hormone auxin are associated with growth responses in roots.

Auxin Regulates SYP132 Expression and Influences Root Growth

Auxin differentially regulates *SYP132* expression in shoot and root tissue (Xia et al., 2019). In shoots, auxin reduces SYP132 expression and endocytic traffic associated with this SNARE, thereby increasing PM H^+-ATPase density and promoting shoot growth. To determine how auxin affects SYP132 expression in roots, we used Arabidopsis seedlings expressing GFP-fused SYP132 under the *SYP132* native promoter (*SYP132p*::GFP-SYP132; Ichikawa et al., 2014). Auxin analog 1-Naphthalene-acetic acid (NAA) was used in these experiments as it is stable and efficiently penetrates cells (Delbarre et al., 1996). Seedlings were grown on half-strength Murashige and Skoog (0.5× MS) media and infiltrated with auxin (NAA, 10^{-6} M) or 0.02% (v/v) ethanol in water (control). Roots were separated from shoots and sampled at different time points after auxin treatment for immunoblot analysis using anti-GFP antibodies (Fig. 1A). We found, following auxin treatment, that SYP132 protein levels initially declined over the first 30 min of auxin treatment, but within 60 min SYP132 expression recovered and, after 240 min, SYP132 levels were higher compared with the control (Fig. 1, A and B). GFP-SYP132 protein quantity was calculated for each time point using densitometric quantification of bands and normalized to the total protein per lane (Fig. 1B).

Exogenous auxin treatment is known to suppress root growth in a dose-dependent manner (Rahman et al., 2007). To test how SYP132 influences root growth, we analyzed main root length. In the absence of a viable homozygous *syp132* mutant (Park et al., 2018), root growth in Arabidopsis lines constitutively over-expressing SYP132 (SYP132-OX, 35S::RFP-SYP132, Xia et al., 2019) were compared against wild-type plants. Seedlings were grown on 0.5× MS plates for 5 d before measurements (Fig. 1C). We found that SYP132-OX

[1]This work was supported by the Royal Society (University Research Fellowship UF150364, Research Grant RG160493; to R.K.) and the Biotechnology and Biological Sciences Research Council (BBSRC) (BB/S017348/1; to R.K.), the China Scholarship Council (CSC) (to L.X.; a Ph.D. studentship), and the University of Glasgow Leadership funds (to R.K.).

[2]These authors contributed equally to this work.

[3]Present address: Department of Molecular Genetics, Centre for Research in Agricultural Genomics (CRAG), Campus UAB Bellaterra, Cerdanyola del Vallès 08193, Barcelona, Spain

[4]Author for contact: rucha.karnik@glasgow.ac.uk.

[5]Senior author.

The author responsible for distribution of materials integral to the findings presented in this article in accordance with the policy described in the Instructions for Authors (www.plantphysiol.org) is: Rucha Karnik (rucha.karnik@glasgow.ac.uk).

L.X. carried out main root growth and protein biochemistry; L.X. and M.M.-B. carried out gravitropism experiments and transcript analysis; all authors did data analysis; R.K. conceptualized the project, planned experiments, and wrote the manuscript.

[OPEN]Articles can be viewed without a subscription.

www.plantphysiol.org/cgi/doi/10.1104/pp.19.01301

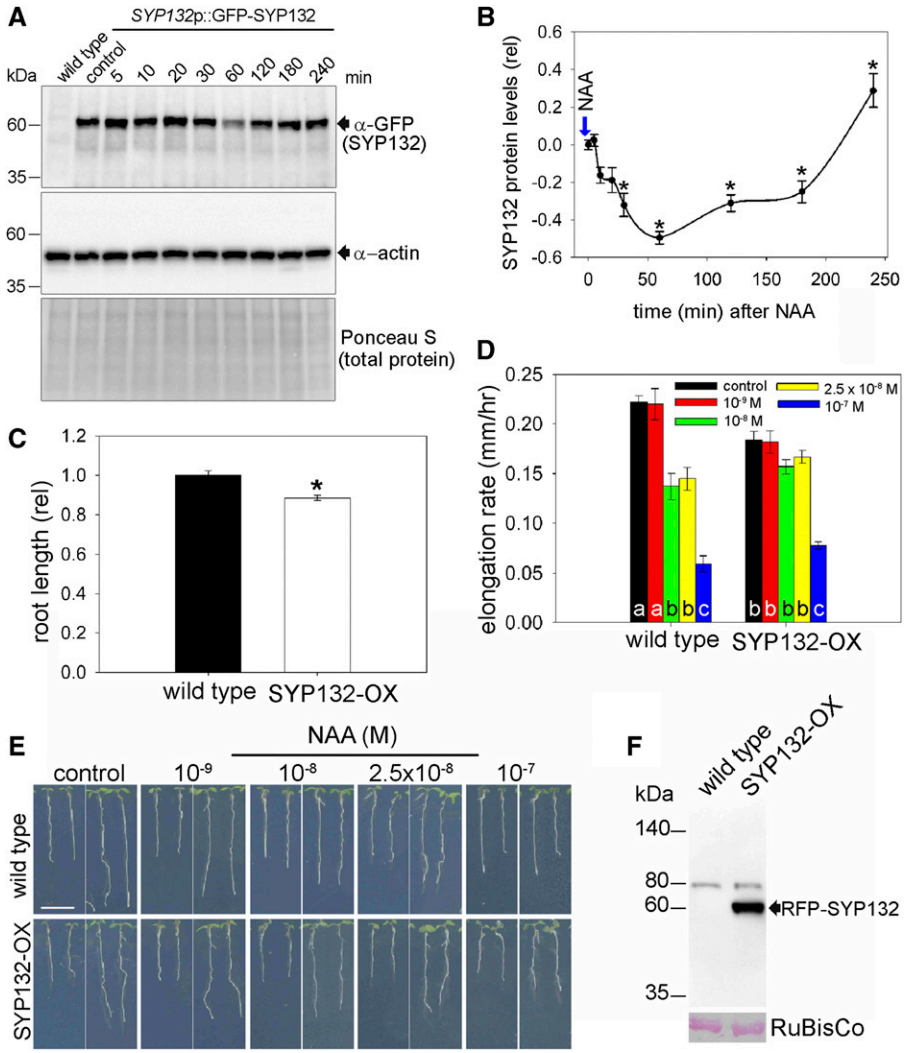

Figure 1. Auxin regulates SNARE SYP132 abundance during root growth. A, Immunoblot analysis of separated root tissue following treatment with 10^{-6} M NAA (auxin) for up to 240 min. Seedlings were grown on 0.5× MS plates for 3 weeks before treatment. Total protein was resolved on a single gel (10%, SDS-PAGE), and immunoblots were performed using anti-GFP (Abcam) to visualize GFP-SYP132 (~62 kD, top) and antiactin (Agrisera) to detect reference protein actin (~45 kD, middle). Black arrows indicate the expected band position. Ponceau S staining (bottom) was used to detect total protein on the membrane. B, Graph showing relative change in GFP-SYP132 protein expression compared with 0.02% (v/v) ethanol in water (control), calculated by densitometric analysis of immunoblots using Fiji software and normalized to total protein in each lane. Data are mean ± SE; $n = 3$ experiments. C, Main root lengths of 3-d-old wild type and SYP132-OX Arabidopsis seedlings. Data are mean ± SE, relative to wild type. Asterisk indicates statistical significance using ANOVA (*$P < 0.05$), $n \geq 300$. D, Root growth rates in wild type and SYP132-OX seedlings in response to treatment with auxin at different concentrations. Seedlings were germinated on 0.5× MS plates, and after 5 d they were transferred to 0.5× MS plates containing 0 (control), 10^{-9}, 10^{-8}, 2.5×10^{-8}, and 10^{-7} M NAA (auxin). Main root growth rates, in millimeters per hour, were calculated over 48 h. Data are mean ± SE ($n \geq 50$ roots, from three independent experiments). Statistical significance using ANOVA is indicated by letters ($P < 0.001$). E, Representative images of Arabidopsis seedlings at 0 and 48 H, as described in D. Scale bar = 1 cm. F, Immunoblot analysis using anti-RFP (top) to detect RFP-SYP132 (~61 kD) protein expression in the Arabidopsis SYP132-OX line. Ponceau S staining of Rubisco was used as loading control (bottom).

seedlings had shorter root lengths compared with the wild type (Fig. 1C). We also tested the effect of SYP132 in auxin-associated root growth. Arabidopsis seedlings grown on 0.5× MS plates were transplanted to plates supplemented with increasing concentrations of NAA, and root elongation rates were measured over 48 h (Fig. 1, D–F). In wild-type Arabidopsis roots, 10^{-9} M NAA had no significant effect on root growth, but as the NAA concentration was raised (10^{-8} M and 2.5×10^{-8} M NAA), root growth rates decreased. We carried out parallel measurements with SYP132-OX roots. As expected, in the absence of auxin supplementation, we observed reduced elongation rates compared with the wild-type plants. However, increasing NAA had no

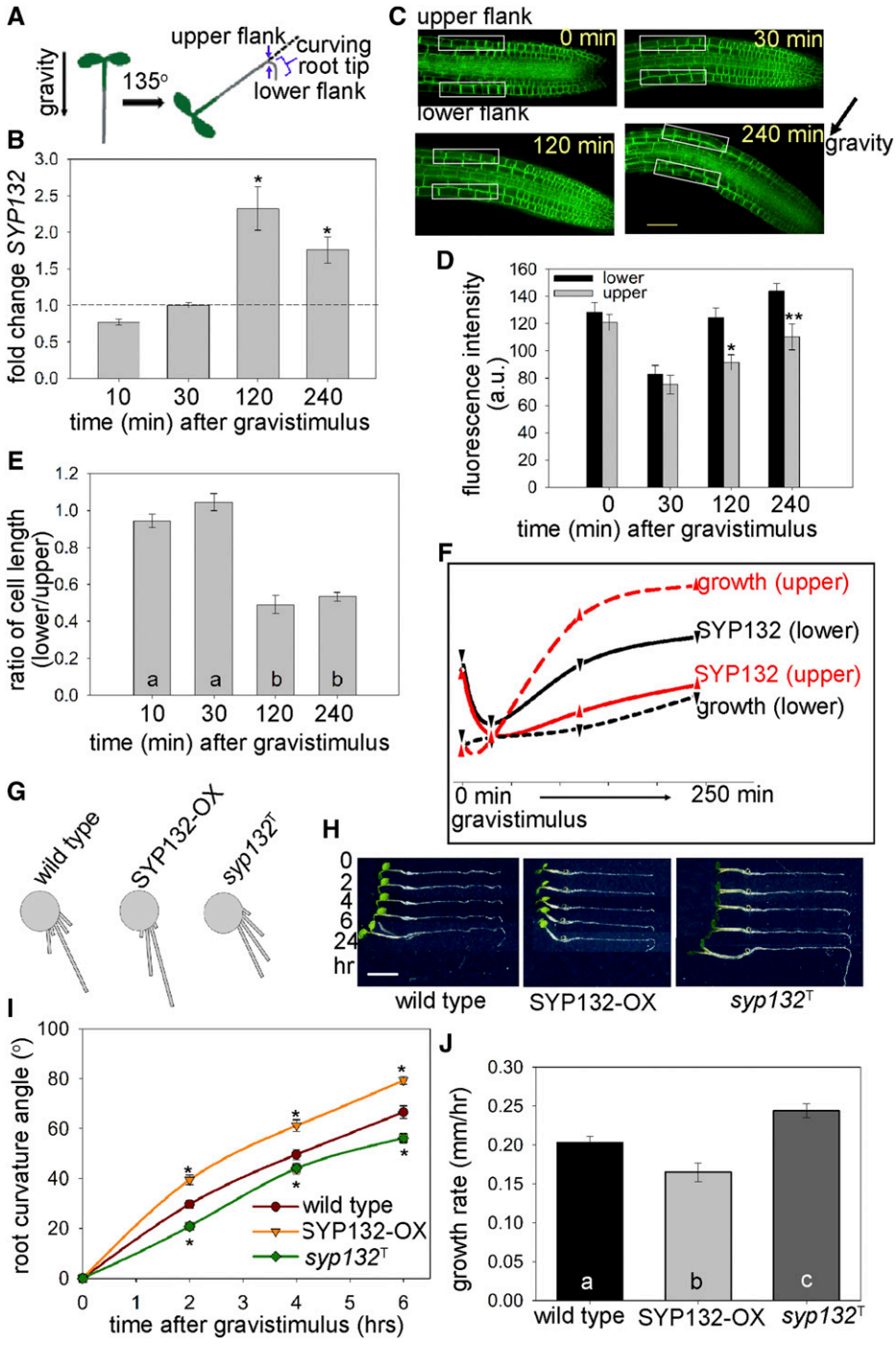

Figure 2. Auxin regulates SNARE SYP132 abundance during root gravitropism. A, Schematic representation of gravitropic stimulation of root tips. B, Fold changes in *SYP132* transcript levels in gravistimulated root tips at different time points. Wild-type seedlings were grown vertically on 0.5× MS media for 6 d after which the plates were turned at an angle of 135° and root tips were excised and collected at 0, 10, 30, 120, and 240 min after gravistimulation. Fold changes in gene expression with reference to time 0 were calculated as $2^{-\Delta\Delta CT}$ (Livak and Schmittgen, 2001). The mitochondrial 18S rRNA gene (*AtMg01390*) was used as a control. Asterisk indicates statistical significance calculated using ANOVA (*$P < 0.050$); $n = 3$. C, Representative confocal images of the midsection of *SYP132*p::GFP-SP132 Arabidopsis root tips, gravistimulated (135°) for 0, 30, 120, and 240 min. Boxed areas represent parts of the elongation zone used for fluorescence analysis. Arrow represents the direction of the gravity vector. Scale bar = 50 μm. D, GFP-SYP132 expression in top and bottom flanks of gravistimulated roots marked in (C). Data are mean of fluorescence intensities measured using Fiji software. Asteriks indicate statistical significance between each top and bottom flank values is calculated using ANOVA (*$P < 0.001$ and **$P < 0.001$); $n = 6$. A.u., arbitrary units. E, Mean cell length ratios for bottom and top flanks of the roots ± SE. Length of cells on opposite ends of gravistimulated roots represented in (C) were

additional effect on root growth even at a higher concentration range of 10^{-8} and 2.5×10^{-8} M (Fig. 1, D and E). Very high auxin (10^{-7} M NAA) severely inhibited root growth. We noted that auxin did not alter RFP-SYP132 protein levels in SYP132-OX plants (Xia et al., 2019), which discounts the possibility that auxin regulates the SNARE through additional pathways such as degradation. Instead, these observations are most easily explained as a result of saturation of SYP132 expression and masking of the auxin dose-dependence in root growth in the SYP132-OX plants (Fig. 1, D and E). Regardless of the interpretation, however, these findings support the involvement of SYP132 in auxin-mediated root growth responses.

SYP132 Contributes to Differential Root Growth Responses and Gravitropic Curvature

Auxin regulates plant gravitropic root growth responses through a complex set of molecular mechanisms (Su et al., 2017). Upon gravistimulation (see schematic, Fig. 2A), auxin gradients are generated across the top and bottom flanks of the root, which drive root growth responses. Auxin levels are higher on the bottom flank of the root, where cell elongation is reduced, compared with the top flank, and these differences in growth result in curvature of the root toward the Earth's gravity vector (Swarup et al., 2005; Monshausen et al., 2011; Velasquez et al., 2016; Barbez et al., 2017; Su et al., 2017).

To test the role of the SNARE SYP132 in gravitropic growth, a gravistimulus was applied to wild-type Arabidopsis roots by rotating plants grown on plates to 135° (Fig. 2A). It is not possible to effectively segregate tissue from the top and bottom flanks of the root tip. Therefore, total root tip tissue was collected at different time points and was analyzed for *SYP132* transcript levels by reverse transcription quantitative PCR. During phase 1 of the gravitropic response, an auxin gradient is generated across the root tip and initiates auxin-regulated transcriptional changes and differential growth. Subsequently, auxin asymmetry is lost. Phase 2 follows after approximately 100 min during which the downstream targets or effectors continue to contribute to growth for gravitropic curvature of the root in the absence of an auxin gradient (Band et al., 2012). We observed SYP132 expression in gravistimulated root tips to follow this second phase of growth (Fig. 2B). During the first 30 min after stimulus, total root tip *SYP132* transcript levels did not change, but after 120 min, total root tip *SYP132* transcripts were higher relative to those at the start of the stimulus (Fig. 2B). Such an increase in total root tip *SYP132* levels would underestimate local increase of the SNARE within regions of the root tip.

To understand how changes in *SYP132* transcripts correlate with SYP132 protein distribution, confocal imaging of gravistimulated *SYP132*p::GFP-SP132 Arabidopsis root tips (Ichikawa et al., 2014) were performed. The GFP fluorescence intensity in root cells lining the top and bottom flanks of the root elongation zone was measured at different time points (Fig. 2C). GFP-SYP132 fluorescence intensity was similar in the top and bottom flanks of the roots at 0 and 30 min after stimulus, but after 120 min, GFP-SYP132 fluorescence at the top flank was reduced compared with the bottom flank (Fig. 2D). This unequal distribution of GFP-SYP132 complemented the differential in cell expansion determined by changes in the cell-length ratio for cells lining the lower flank compared with those lining the top flank (Fig. 2E). Differential in SYP132 expression aligns inversely with growth in the top and bottom flanks of the root (Fig. 2F).

Finally, to explore the physiological role of SYP132 in gravitropic growth, we measured the angle of curvature and growth rates of gravistimulated root tips in wild-type, SYP132-OX, and heterozygous *SYP132* transfer (T) DNA insertion mutant (*syp132*^{T}) Arabidopsis seedlings (Fig. 2, G–J), of which the latter have a 5-fold reduction in SYP132 expression (Xia et al., 2019). When compared with the wild type, the SYP132-OX lines showed increased gravitropic curvature and a reduced root growth rate over 24 h. Conversely, in the heterozygous *syp132*^{T} mutants, gravitropic curvature was reduced, but root growth rate was higher (Fig. 2, G–J). We understand the difference between the wild type, SYP132-OX, and *syp132*^{T} mutants in gravistimulated roots assuming that auxin evokes finite changes in SYP132 expression. Key to this interpretation is a recognition that SYP132 suppresses cell elongation, thus reducing the rate of growth. Gravistimulation evokes radial auxin gradients that associate with a differential in SYP132 expression across the top and bottom flanks of the root tip. Where SYP132 expression increases,

Figure 2. (*Continued.*)
measured from confocal images using Fiji. Statistical significance using ANOVA is indicated by letters ($P < 0.001$); $n \geq 20$. F, Schematic representation of SYP132 protein levels (bold lines) in top (red lines) and bottom (black lines) flanks and corresponding changes in growth (dashed lines), referenced from cell lengths in gravistimulated roots over 240 min. Schematic represents data in (C) to (E). G, Gravitropism diagram representing distribution of root curvature angles following 6 h of gravistimulation, each assigned to one of eight 45° sectors. The lengths of the bars in the diagram represent the percentage of wild type, SYP132-OX, and *syp132*^{T} seedlings occurring in each assigned sector. H, Images from the same wild type, SYP132-OX, and *syp132*^{T} seedlings following gravistimulation, as in (A), acquired at different time points. Images are representative of $n = 5$ independent experiments. Bar = 5 mm. Hr, hour. I, Root curvature angle after gravistimulation over 6 H, depicting reoriented root tip growth toward the Earth's gravity vector. Data are mean ± SE ($n \geq 50$ roots, from three independent experiments). Asterisk indicates statistically significant differences for each time point compared with the wild type using ANOVA (*$P < 0.001$). J, Bar graph depicting growth rate of roots after gravistimulation, measured over 24 h. Data are mean ± SE. Letters indicate statistical significance using ANOVA ($P < 0.050$); $n \geq 30$ roots, from three independent experiments.

growth is reduced. Overexpressing this SNARE elevates background SYP132 protein abundance and reduces overall growth. It follows that in the SYP132-OX line, the differential in growth is enhanced and gravitropic curvature is more pronounced. Conversely, in the *syp132*^{T} mutant, background SYP132 protein abundance is lower, the overall growth rate is higher, and there is less curvature (Fig. 2, H–J).

There is evidence for auxin in apoplastic pH regulation mediated through plasma membrane H^+-ATPase (Fasano et al., 2001; Barbez et al., 2017). We suggest that these same features may be responsible for the asymmetric ion fluxes that drive root cell expansion and gravitropism. Our data align with the role of SYP132 and associated traffic on plasma membrane H^+-ATPase endocytosis and consequent decrease in function of the proton pump in the shoot tissue (Xia et al., 2019). In conclusion, we propose that auxin regulates the SNARE SYP132 during root growth and gravitropic responses and that hormone-regulated membrane traffic associated with this SNARE is important for understanding of auxin-associated growth.

Received November 20, 2019; accepted January 13, 2020; published January 23, 2020.

Lingfeng Xia[2]
ORCID ID: 0000-0002-8628-8062
Plant Science Group, Laboratory of Plant Physiology and Biophysics, Institute of Molecular, Cell and Systems Biology, University of Glasgow, Glasgow G12 8QQ, United Kingdom

Maria Mar Marquès-Bueno[2,3]
ORCID ID: 0000-0003-3178-1922
Plant Science Group, Laboratory of Plant Physiology and Biophysics, Institute of Molecular, Cell and Systems Biology, University of Glasgow, Glasgow G12 8QQ, United Kingdom

Rucha Karnik[4,5]
ORCID ID: 0000-0001-6876-4099
Plant Science Group, Laboratory of Plant Physiology and Biophysics, Institute of Molecular, Cell and Systems Biology, University of Glasgow, Glasgow G12 8QQ, United Kingdom

LITERATURE CITED

Band LR, Wells DM, Larrieu A, Sun J, Middleton AM, French AP, Brunoud G, Sato EM, Wilson MH, Péret B, et al (2012) Root gravitropism is regulated by a transient lateral auxin gradient controlled by a tipping-point mechanism. Proc Natl Acad Sci USA **109:** 4668–4673

Barbez E, Dünser K, Gaidora A, Lendl T, Busch W (2017) Auxin steers root cell expansion via apoplastic pH regulation in *Arabidopsis thaliana*. Proc Natl Acad Sci USA **114:** E4884–E4893

Delbarre A, Muller P, Imhoff V, Guern J (1996) Comparison of mechanisms controlling uptake and accumulation of 2,4-dichlorophenoxy acetic acid, naphthalene-1-acetic acid, and indole-3-acetic acid in suspension-cultured tobacco cells. Planta **198:** 532–541

Enami K, Ichikawa M, Uemura T, Kutsuna N, Hasezawa S, Nakagawa T, Nakano A, Sato MH (2009) Differential expression control and polarized distribution of plasma membrane-resident SYP1 SNAREs in Arabidopsis thaliana. Plant Cell Physiol **50:** 280–289

Fasano JM, Swanson SJ, Blancaflor EB, Dowd PE, Kao TH, Gilroy S (2001) Changes in root cap pH are required for the gravity response of the Arabidopsis root. Plant Cell **13:** 907–921

Guilfoyle TJ, Hagen G, Li Y, Gee MA, Martin G, Ulmasov TN (1992) Transcriptional regulation of auxin-responsive genes. Progress in Plant Growth Regulation **13:** 128–135

Haswell ES (2003) Gravity perception: How plants stand up for themselves. Curr Biol **13:** R761–R763

Ichikawa M, Hirano T, Enami K, Fuselier T, Kato N, Kwon C, Voigt B, Schulze-Lefert P, Baluška F, Sato MH (2014) Syntaxin of plant proteins SYP123 and SYP132 mediate root hair tip growth in Arabidopsis thaliana. Plant Cell Physiol **55:** 790–800

Karnik R, Waghmare S, Zhang B, Larson E, Lefoulon C, Gonzalez W, Blatt MR (2017) Commandeering Channel Voltage Sensors for Secretion, Cell Turgor, and Volume Control. Trends Plant Sci **22:** 81–95

Livak KJ, Schmittgen TD (2001) Analysis of relative gene expression data using real-time quantitative PCR and the $2(-^{\Delta\Delta C_T})$ method. Methods **25:** 402–408

Monshausen GB, Miller ND, Murphy AS, Gilroy S (2011) Dynamics of auxin-dependent Ca^{2+} and pH signaling in root growth revealed by integrating high-resolution imaging with automated computer vision-based analysis. Plant J **65:** 309–318

Park M, Krause C, Karnahl M, Reichardt I, El Kasmi F, Mayer U, Stierhof YD, Hiller U, Strompen G, Bayer M, et al (2018) Concerted action of evolutionarily ancient and novel SNARE complexes in flowering-plant cytokinesis. Dev Cell **44:** 500–511.e4

Rahman A, Bannigan A, Sulaman W, Pechter P, Blancaflor EB, Baskin TI (2007) Auxin, actin and growth of the Arabidopsis thaliana primary root. Plant J **50:** 514–528

Su SH, Gibbs NM, Jancewicz AL, Masson PH (2017) Molecular mechanisms of root gravitropism. Curr Biol **27:** R964–R972

Swarup R, Kramer EM, Perry P, Knox K, Leyser HM, Haseloff J, Beemster GT, Bhalerao R, Bennett MJ (2005) Root gravitropism requires lateral root cap and epidermal cells for transport and response to a mobile auxin signal. Nat Cell Biol **7:** 1057–1065

Velasquez SM, Barbez E, Kleine-Vehn J, Estevez JM (2016) Auxin and cellular elongation. Plant Physiol **170:** 1206–1215

Xia L, Mar Marquès-Bueno M, Bruce CG, Karnik R (2019) Unusual roles of secretory SNARE SYP132 in plasma membrane H^+-ATPase traffic and vegetative plant growth. Plant Physiol **180:** 837–858